RSC Advances

Predicting the Optimum Compositions of a Parenteral Nanoemulsion System Loaded with Azithromycin Antibiotic Utilizing Artificial Neural Network Model

Journal:	*RSC Advances*
Manuscript ID:	RA-ART-07-2015-014913.R1
Article Type:	Paper
Date Submitted by the Author:	23-Aug-2015
Complete List of Authors:	Albana, Ghaidaa; Universiti Putra Malaysia, Medicine Department Basri, Hamidon; Universiti Putra Malaysia, Medicine Stanslas, Johnson; Universiti Putra Malaysia, Medicine Fard Masoumi, Hamid Reza; Universiti Putra Malaysia, Chemistry BASRI, MAHIRAN; UNIVERSITI PUTRA MALAYSIA,

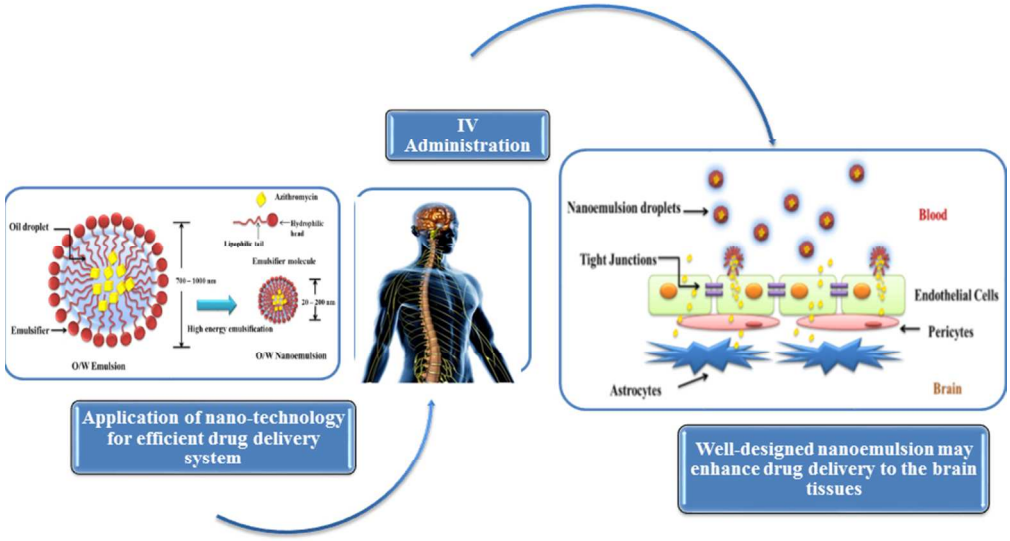

254x190mm (96 x 96 DPI)

RSC. Advances

ARTICLE

Predicting the Optimum Compositions of a Parenteral Nanoemulsion System Loaded with Azithromycin Antibiotic Utilizing Artificial Neural Network Model

Received 00th January 20xx,
Accepted 00th January 20xx

DOI: 10.1039/x0xx00000x

www.rsc.org/

Ghaidaa S. Daood[a], Hamidon Basri [a, b]*, Johnson Stanslas[a, b], Hamid Reza Fard Masoumi[c] and Mahiran Basri[c, d]

For the purpose of brain delivery via intravenous administration, formulation of azithromycin- loaded nanoemulsion system was optimized utilizing artificial neural network (ANN) as a multivariate statistical technique. The input effective variables for nanoemulsion formulation were drug loading, Surfactant and co-surfactant content, concentration of glycerol, and vitamin E while the particle size was the output response since the size reduction will improve the stability of nanoemulsion and the biological efficacy of the drug *in-vivo* after parenteral administration. To achieve the optimum topologies; ANN was trained by Incremental Back-Propagation (IBP), Batch Back-Propagation (BBP), Quick Propagation (QP), and Levenberg-Marquardt (LM) algorithms for testing data set. The topologies were confirmed by the indicator of minimized root mean squared error (RMSE) for each. Based on that indicator; the BBP-5-14-1 was selected as the optimum topology to be used as a final model to predict the desirable particle size and relative importance of the formulation's effective variables. The ANN analysis showed that the actual particle size (54.7 nm ± 0.8) of the formulated nanoemulsion was quite close to the predicted value (53.9 nm) obtained from batch back propagation-ANN model which support the conclusion that ANN model has the potential to predict a stable nanoemulsion system that could be used efficiently for parenteral administration of azithromycin antibiotic.

Introduction

Azithromycin(9-deoxo-9a-aza-9a-methyl-9a-homoerthromycin) is a semi-synthetic antibiotic "derived from the naturally occurring antibiotic erythromycin" representing the first of a subclass of macrolides classified as azalides [1]. It was first produced in 1980's by the insertion of methyl-substituted nitrogen on the lactone ring of erythromycin at position 9a **(Fig. 1)** creating a 15-membered macrolide.

This alteration increases the stability of the compound in acidic media and subsequently improving its oral bioavailability compared to erythromycin and it provides a larger spectrum of activity against Gram-negative bacteria as well [2]. Azithromycin has a unique pharmacokinetic profile that distinct it from macrolides and other antibiotics, it is a tissue selective antibiotic [3] that can achieve high cellular concentrations after administration and subsequent slow, sustained release into the blood stream which results in therapeutic level of the drug being maintained for several days in the tissues, thus enabling the drug to be given once daily over a short course treatment regimen of 3-5 days.

Bacterial meningitis (BM) is an acute infection of the protective membranes surrounding the brain (meninges) [4] which is followed by a central nervous system (CNS) inflammatory reaction that causes coma, seizure activity, increased intracranial pressure and stroke or even death [5]. BM is a serious threat to global health accounting for an estimated 171000 deaths worldwide per year [6]. It is fatal in 50% of the cases if untreated, even when the disease is diagnosed early and adequate treatment is started, 5-10% of patients die, typically within 24-48 h after the onset of symptoms [7].

[a.] *Department of Medicine, Faculty of Medicine and Health Sciences, Universiti Putra Malaysia, 43400, Serdang, Selangor, Malaysia*
[b.] *Laboratory of Pharmacotherapeutics, Faculty of Medicine and Health Sciences, Universiti Putra Malaysia, 43400,Serdang, Selangor, Malaysia*
[c.] *Department of Chemistry, Faculty of Science, Universiti Putra Malaysia, 43400, Serdang, Selangor, Malaysia*
[d.] *Laboratory of Molecular Biomedicine, Institute of Bioscience, Universiti Putra Malaysia, 43400,Serdang, Selangor, Malaysia*

***Corresponding author:**
Prof. Dr. HJ. Hamidon Basri
Deputy Dean (Academic: Medicine)
Faculty of Medicine & Health Science
Universiti Putra Malaysia
43400 UPM Serdang
Selangore, Darul Ehsan
Telephone number: +603-8947 2607/2608
Fax number: +603-8947 2585
E-mail address: hamidon@medic.upm.edu.my

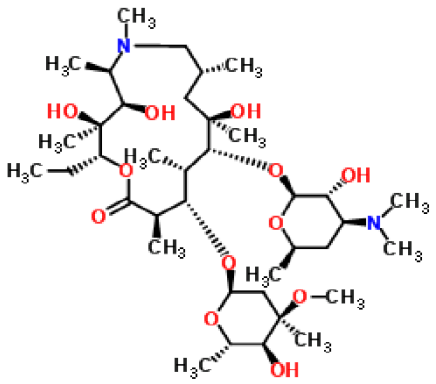

Fig.1: The chemical structure of azithromycin antibiotic

Despite advances in antibacterial therapy and vaccine development, BM constitutes a significant cause of morbidity and mortality, mostly in pediatric patients. Several antibiotics have been used for the treatment of meningitis (e.g. ampicillin, ceftriaxone, vancomycin, gentamycin), but the continuous increase in the number of infections caused by bacteria resistant to one or more antibiotic classes represents a serious threat as it may lead to treatment failures. Although resistance cannot be prevented, but its development and spread can be slowed, one of the tools is maximizing diversity in the prescription of the treatment regimen [8].

Despite the fact that azithromycin is highly effective against two out of the three main causative agents of bacterial meningitis (*Haemophilusinfluenzae* (*H. influenzae*) type b (Hib) and *Streptococcus pneumonia* (*S. pneumoniae*)) [9], it cannot be used for the treatment of meningitis because it doesn't possess the appropriate physicochemical criteria that enables it to penetrate the blood brain barrier (BBB) which encapsulate the brain. Though it is lipophilic but it is a large molecule with a molecular weight of 749 Da. The presence of the BBB represents a big challenge for effective delivery of therapeutics to the brain. The BBB acts very effectively to protect the brain from common pathogens circulating in the blood [10], thus infections of the brain are not very common. However, since antibodies and antibiotics are too big to cross the BBB, infections that do occur are often very serious and too difficult to treat. Incorporating azithromycin in the oil core of a nanoemulsion system will protect the drug from being metabolized early by the hepatic enzymes, thereby increasing the circulation time of the drug in the blood stream and consequently will increasing the probability of its arrival to the brain. Making an advantage of the nanosized molecule, the drug may permeate the BBB and reach the meninges in adequate quantities to produce its therapeutic effect.

Optimizing the effective variables; percentage of azithromycin, lecithin, Tween 80, glycerol, and vitamin E, appears curtail to minimize the particle size and maximize the stability of the nanoemulsion system. Since, nanoemulsion is a multivariate system during performance; the traditional optimization techniques such as one-variable-at-a-time method may involve a higher number of experimental trials to evaluate the interaction between the independent variables and the response [11]. Furthermore, it does not consider the potential interaction between the affecting variables which might leads to sub-optimal results[12]. On the other hand, the multivariate methods have been widely applied for the modeling of input effective variables to optimize the compositions of nanoemulsion system as output [13]. One of the multivariate methods is artificial neural networks (ANNs) that models the interaction of the variables simultaneously during the performance by using universal mathematical learning algorithms. The algorithms are Incremental Back-Propagation, Batch Back-Propagation, Quick Propagation, and Levenberg-Marquardt [14]. The artificial neural networks have been used for representing non-linear functional relationships between variables. The ability of an ANN to learn and generalize the behavior of any complex and non-linear process makes it a powerful modeling tool. Solving and modeling the complex relation between input and output variable can be simply performed by an ANN model imitated by biological neuron processing. The generated model is used to predict the importance and the optimum value of each variable in the multivariate formulation process. In this research, the percentage of nanoemulsion compositions [drug (azithromycin), surfactant (lecithin), co-surfactant (Tween 80), glycerol, and antioxidant (vitamin E)] were modeled as effective variables by the multilayer feed-forward neural network. To obtain the appropriate model, the network was trained by using IBP, BBP, QP, and LM learning algorithms. The optimum topologies of each algorithm were determined by minimizing root mean squared error (RMSE) [15].

The performance of the obtained topologies was compared by minimized absolute average deviation (AAD) and maximized R-squared (R^2) to select the final optimum model of the nanoemulsion system. The model was used to determine the importance and narrow levels of the effective variable. Moreover, the appropriate particle size of the nanoemulsion was predicted at the optimum conditions [16].

Experiment
Materials and methods

Materials

Soya bean oil was obtained from Sigma- Aldrich Chemie GmbH, Germany. The main unsaturated fatty acids in soya bean oil triglycerides are the poly-unsaturates, alpha-linolenic acid (C-18:3); 7-10%, and linoleic acid (C-18:2); 51%, and the mono-unsaturate, oleic acid (C-18:1); 23%. It also contains the saturated fatty acids, stearic acid, (C-18:0); 4%, and palmitic acid, (C-16:0); 10%. A lipophilic surfactant; pure soya bean lecithin with 70% phosphatidylcholine (Lipoid S75) was purchased from Lipoid GmbH, Ludwigshafen-Germany. The non-ionic surfactant Tween 80 (polyoxyethylene sorbitan monooleate), Oleic acid, Vitamin E were purchased from Fluka, Sigma- Aldrich Chemie GmbH, Germany. Glycerol was purchased from JT Baker, USA. Azithromycin **(Fig. 1)** was purchased from Euroasian Chemicals Private limited, India.

Water that was used as an aqueous phase for the nanoemulsion system, was deionized by Milli-Q filtration system, USA.

The modeling and optimizing of nanoemulsion system was carried out using Neural Power software version 2.5. To design the experiments, the levels of the effective input variables were considered such as azithromycin (0.8- 1.6 %), lecithin (0.5- 2 %), Tween 80 (0.6- 2 %), glycerol (0- 2.75 %), vitamin E (0- 0.25 %) while the particle size was the interested response **(Table 1)**. As shown in **Table 1**, the total of 39 experiment points have been randomly divided into two data sets, training set (32 points) and testing set (7 points). The measurements were conducted in duplicate to donate standard deviations. The software facilitates the option of randomization, the training and testing data sets were used to compare and ensure robustness of the network parameters, respectively. Moreover, the testing set was utilized to avoid over fitting by controlling errors. Additionally, the validation data set (6 points) which was excluded from training and testing sets, evaluates the predictive ability of the generated model **(Table 2)**.

Formulation of nanoemulsion system

According to the experimental design, nanoemulsion was prepared using different types of emulsification method; low energy and high energy emulsification. The oil phase (which consist of soya bean oil and oleic acid as the oil core; Tween 80 and lecithin as the surfactant mixture; azithromycin antibiotic, and vitamin E as an antioxidant) was titrated drop wise into the aqueous phase (which was prepared by dissolving glycerol that serves as a co-surfactant and an isotonic agent in the deionized water). The coarse emulsion that was formed using the overhead stirrer (Stirrer RW16 Basic IKA®, USA) for 30 minutes at 300- 310 rpm, and it was further homogenized using high shear homogenizer (PT3100 High Shear Homogenizer, POLYTRON, Kinematica AG, Switzerland) for 20 minutes at 4000 rpm. The emulsion was then subjected to high pressure homogenization (GEA NiroSoavi NS1001L2K, GEA NiroSoavi, Italy) at 1000 bar for 8 cycles to produce the nano-sized emulsion. The temperature of the whole homogenization process was maintained below 40°C using ice-water bath. The actual particle size for the formulated nanoemulsions was measured by dynamic light scattering (DLS) with an angle of 137° at room temperature of 25°C using Malvern Nano ZS90 apparatus (Malvern, UK).

The ANN description

Artificial neural networks which consist of input, hidden and output layers are mathematic free functionalization of the complicated practical process. The layers which contain several nodes, are connected by multilayer normal feed-forward or feed-back connection formula. The hidden layer could be more than one parallel layer, however the single hidden layer is universally suggested. The connection in such a way that the nodes of particular layer are connected to the nodes of the next layer [15]. The qualification is carried out by associated weights during learning process by well-known learning algorithms.

The learning process

In the learning process, the weights are calculated by the weighted summation of the received data from the former layer and transfer the next layer. The universal learning algorithms are IBP, BBP, QP, GA, and LM while the multilayer is the nodes' connection type [16]. The scaled data will be passed into the first layer, propagated to the hidden layer and finally meet the output layer of the network. Each node in the hidden layer or in output layer acts as a summing junction which modifies the inputs from the previous layer using the following equation:

$$y_i = \sum_{j=1}^{i} x_i \, w_{ij} + b_j \qquad (1)$$

where y_i is the input of the network to j node in hidden layer, i is the number of nodes, x_i is the output of the previous layer while w_{ij} [17] are the weights of connection between the ith node and the jth node. The bias associates with node j is presented by b_j. The main aim of the process is to find the weights for minimizing the error of RMSE which is obtained from the difference between network prediction and actual responses.

$$RMSE = \left(\frac{1}{n} \sum_{i=1}^{n} (y_i - y_{di})^2 \right)^{1/2} \qquad (2)$$

where n is the number of the points, y_i is the predicted value and y_{di} is the actual value. The learning process within an algorithm is continued until finding the minimum RMSE which is known as topology. In order to avoid random correlation due to the random initialization of the weights, learning of a topology is repeated several times. As a net result; the topology with the lowest RMSE is selected to be compared with other nodes' topologies [18]. Following the same manner; the topologies for the n numbers of hidden layer for the specific algorithm are obtained. Finally the topologies of the algorithms are compared to select the provisional model that gives the maximum R^2 (Eq. 3), minimum RMSE and AAD (Eq. 4).

$$R^2 = 1 - \frac{\sum_{i=1}^{n} (y_i - y_{di})^2}{\sum_{i=1}^{n} (y_{di} - y_m)^2} \qquad (3)$$

$$AAD = \frac{1}{n} \sum_{i=1}^{n} \frac{|y_i - y_{di}|}{y_{di}} \times 100 \qquad (4)$$

where n is the number of points, y_i is the predicted value, y_{di} is the actual value and y_m is the average of the actual values.

Table 1: The experimental design that consist of training and testing data sets, each row represents an individual experiment while the columns refer to the compositions of nanoemulsion system. The data are presented as mean ± SD (n=2).

Run No.	*Azithromycin (w/w %)*	*Lecithin (w/w %)*	*Tween 80 (w/w %)*	*Glycerol (w/w %)*	*Vitamin E (w/w %)*	*Particle Size (nm)*	
						Actual	*Predicted*
			Training Set				
1	1.4	2.0	0.6	0	0	94.0 ± 1.8	93.2
2	1.4	2.0	1.0	0	0	100.7 ± 2.3	99.4
3	1.4	2.0	1.2	0	0	104.6 ± 1.2	96.5
4	1.4	2.0	1.8	0	0	85.7 ± 2.6	86.7
5	1.4	2.0	2.0	0	0	82.7 ± 0.9	84.2
6	1.4	1.0	0.6	0	0	89.9 ± 1.4	84.3
7	1.4	1.0	0.8	0	0	82.6 ± 4.6	87.2
8	1.4	1.0	1.4	0	0	73.7 ± 2.6	73.2
9	1.4	1.0	1.6	0	0	67.6 ± 0.7	70.5
10	1.4	1.0	1.8	0	0	71.7 ± 1.1	69.3
11	1.4	1.0	2.0	0	0	69.5 ± 0.9	68.7
12	1.4	1.0	0.6	0	0.25	117.9 ± 1.7	109.0
13	1.4	1.0	0.8	0	0.25	97.7 ± 1.3	103.2
14	1.4	1.0	1.2	0	0.25	89.8 ± 0.8	92.8
15	1.4	1.0	1.8	0	0.25	74.4 ± 2.1	74.1
16	1.4	1.0	2.0	0	0.25	77.6 ± 3.9	73.7
17	1.4	2.0	1.6	0	0.25	77.9 ± 2.7	79.5
18	1.4	2.0	1.6	1.5	0.25	73.0 ± 1.1	71.1
19	1.4	2.0	1.6	2.75	0.25	76.3 ± 2.0	82.7
20	1.4	0.5	1.6	2.5	0.25	102.2 ± 3.1	103.4
21	1.4	2.0	1.6	2.5	0.25	85.2 ± 1.2	80.1
22	1.0	1.0	1.2	2.5	0.25	96.9 ± 4.1	89.0
23	1.6	1.0	1.2	2.5	0.25	82.7 ± 2.3	80.8
24	0.8	1.0	1.0	2.5	0.25	64.6 ± 1.0	68.9
25	1.4	1.0	1.0	2.5	0.25	86.0 ± 1.3	87.0
26	1.0	1.0	2.0	2.5	0.25	59.0 ± 0.7	55.6
27	1.2	1.0	2.0	2.5	0.25	67.8 ± 1.9	70.9
28	1.4	1.0	2.0	2.5	0.25	80.2 ± 1.6	80.5
29	0.8	2.0	2.0	2.5	0.25	50.6 ± 0.5	49.2
30	1.2	2.0	2.0	2.5	0.25	59.2 ± 0.9	59.8
31	1.4	2.0	0.8	0	0	92.4 ± 2.2	98.2
32	1.4	1.0	1.6	2.5	0.25	98.7 ± 2.0	97.2
			Test Set				
1	1.4	2.0	1.4	0	0	93.0 ± 1.4	92.7
2	1.2	1.0	1.2	2.5	0.25	95.8 ± 0.8	95.5
3	1.4	1.0	1.0	0	0	84.7 ± 3.5	85.1
4	1.0	2.0	2.0	2.5	0.25	54.2 ± 1.1	52.0
5	1.4	1.0	1.2	0	0	76.4 ± 0.9	78.7
6	1.4	2.0	1.6	1.0	0.25	71.7 ± 1.6	70.6
7	1.4	2.0	1.6	2.25	0.25	75.6 ± 2.0	77.3

Back Propagation algorithm

In the application of artificial neural network, the BP network and its varied pattern are adopted in most of the neural network models, in fact, BP algorithm is a method to monitor learning [19]. It utilizes the methods of mean square error and gradient descent to realize the modification to the connection weight of network. The modification to the connection weight of network is aimed at achieving the minimum error sum of squares. In this algorithm, a little value is given to the connection value of network first, and then, a training sample is selected to calculate gradient of error relative to this sample. The difference between the real output and expect output of the network is defined as the error signal; in the back propagation of error signal, the error signal is propagated from the output end to the input layer in a layer-by-layer manner. During the back propagation of error signal, the weight value of network is regulated by the error feedback [20]. The continuous modification applied to make the real output of network closer to the expected one. The ideology guiding the learning rules of BP network is: the modification to the weight value and threshold value of network shall be done along the negative gradient direction reflecting the fastest declining of function.

$$x_{k+1} = x_k - \eta_k g_k \qquad (5)$$

where, x_k represents the matrix of current weight value and threshold value; g_k represents the gradient of current function; η_k represents the learning rate [20].

Results and discussion

Modeling process

The topologies of the algorithms

The network of the nanoemulsion system has been organized for five nodes (percentage of each azithromycin, lecithin, Tween 80, glycerol, and vitamin E) in input layer while the particle size of nanoemulsion was the only node in the output layer. The structure of the hidden layer was determined by examining a series of topologies with a range of node number from 1-15 for each individual algorithm. The learning model was performed for testing data set to determine minimum value of RMSE as a function of error [21]. The performance was repeated 10 times for each node to exclude random correlation due to random initialization of the weight. The training was carried out identically for LM, QP, IBP, and BBP algorithms to obtain the optimum topology for each algorithm. Among the 10 times learning replicated data for each node; the minimum value of RMSE was selected and plotted versus the nodes of the algorithms' hidden layer **(Fig. 2)**. As shown, one node out of 15 topologies for each algorithm represented the lowest RMSE and selected as the best topology for comparison. The chosen topologies were 5-7-1, 5-13-1, 5-13-1, and 5-14-1 for LM, QP, IBP, and BBP algorithms, respectively.

Fig. 2 revels that; the topology of BBP-5-14-1 represents the lowest RMSE among the others, thus selected as provisional model for the formulation of nanoemulsion system.

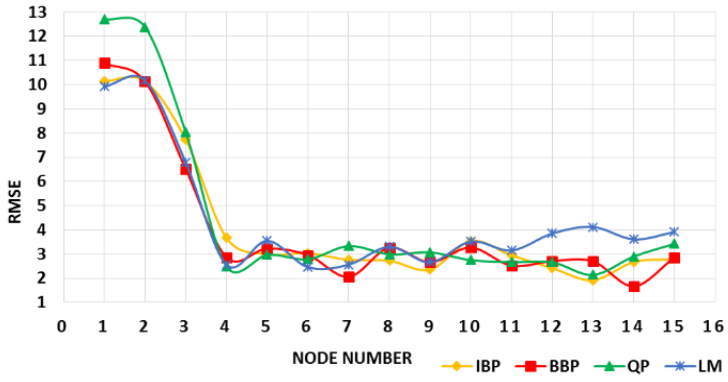

Fig. 2: The selected RMSE vs. node number of the nanoemulsion system network's hidden layers for LM, QP, IBP, and BBP. The lowest RMSE value presented by the node of 7 (LM), 13 (QP), 13 (IBP), and 14 (BBP).

The selection of model

To finalize the model that should be selected for the formulation of nanoemulsion, the values of RMSE, R^2 and ADD were relatively studied for the chosen topology of each algorithm (LM-5-7-1, QP-5-13-1, IBP-5-13-1, and BBP-5-14-1). For the calculation of R^2, the topologies prediction and actual values of nanoemulsion particle size were plotted for testing data set **(Fig.3)** as well as the training set **(Fig. 4)**. As the scatter plots shows, BBP-5-14-1 present the highest R^2 value for testing (0.984) and training (0.930) data sets. The AAD of testing and training sets for those chosen topologies were calculated in **Table 3**. As observed in **Fig. 5**, the lowest value among the AADs belongs to BBP-5-14-1. Having the minimum RMSE and AAD as well as maximum R^2 from all the other topologies for testing data set; BBP-5-14-1 was therefore selected as a final optimum model for the formulation of nanoemulsion system.

Validation of the selected model

The validation of the optimized model was assessed by 6 experimental points which were initially exclude from training and testing data sets (**Table 2**). The results shown in **Table 2** reveal the predicted and actual particle size values. No big differences were noted between the experimentally observed and the predicted particle size values. Additionally, RMSE (1.67) and AAD (1.55) values were quite acceptable to manifest a good predictive accuracy of the model.

Table 2: The validation data set of the effective variables together with actual and predicted particle size of nanoemulsion system.

	Components					*Droplet Size (nm)*		
	AZO %	Lecithin %	Tween 80 %	Glycerol %	Vitamin E %	Actual Value	Predicted Value	RSE %
Validation Set	1.4	2	2	2.5	0.25	54.7 ± 0.8	53.9	1.32
	1.4	1	1.4	0	0.25	84.1 ± 3.6	86.7	2.98
	1.4	2	1.6	2	0.25	72.8 ± 2.1	75.9	4.15
	0.8	1	2	2.5	0.25	49.8 ± 1.9	50.5	1.52
	1.4	2	1.6	0	0	90.9 ± 2.7	89.4	1.64
	1.4	2	1.6	2.5	0.25	77.3 ± 1.1	80.1	3.56

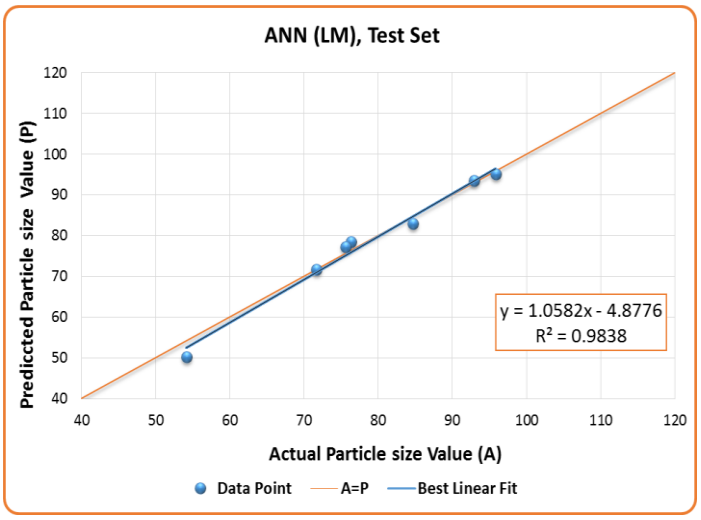

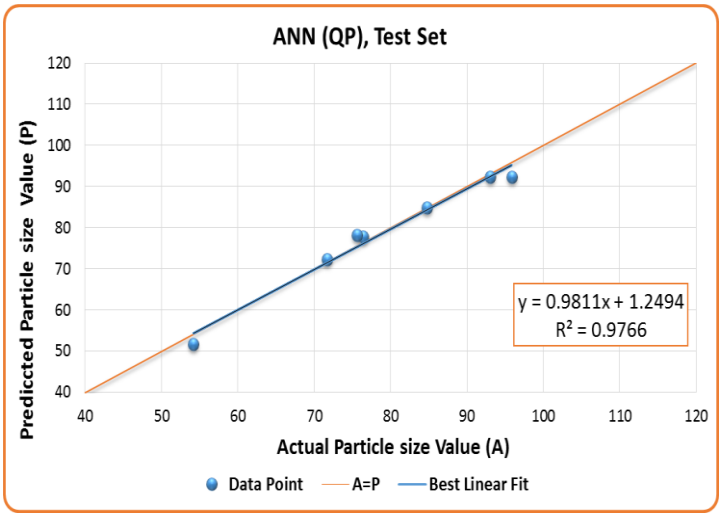

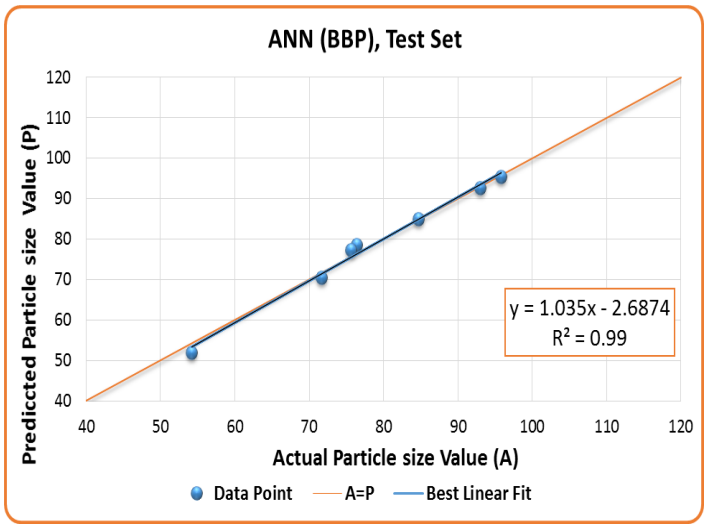

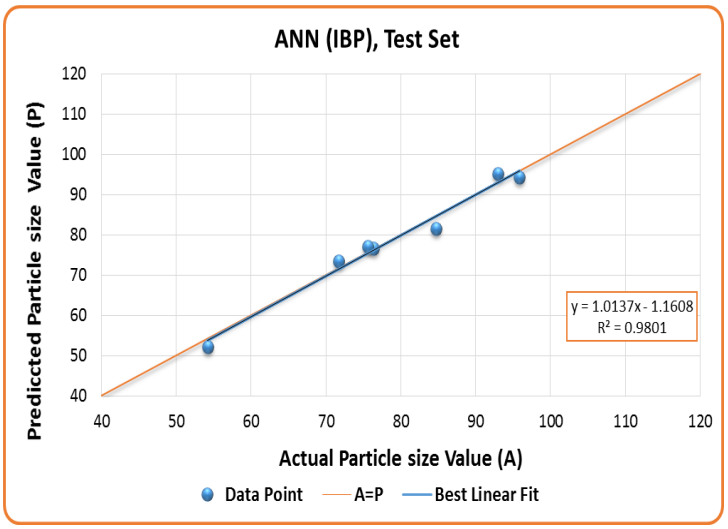

Fig. 3: The scatter plots of the predicted vs. the actual particle size values for the testing data set which show the performed R^2 of the optimized topologies, LM-5-7-1, QP-5-13-1, IBP-5-13-1, and BBP-5-14-1.

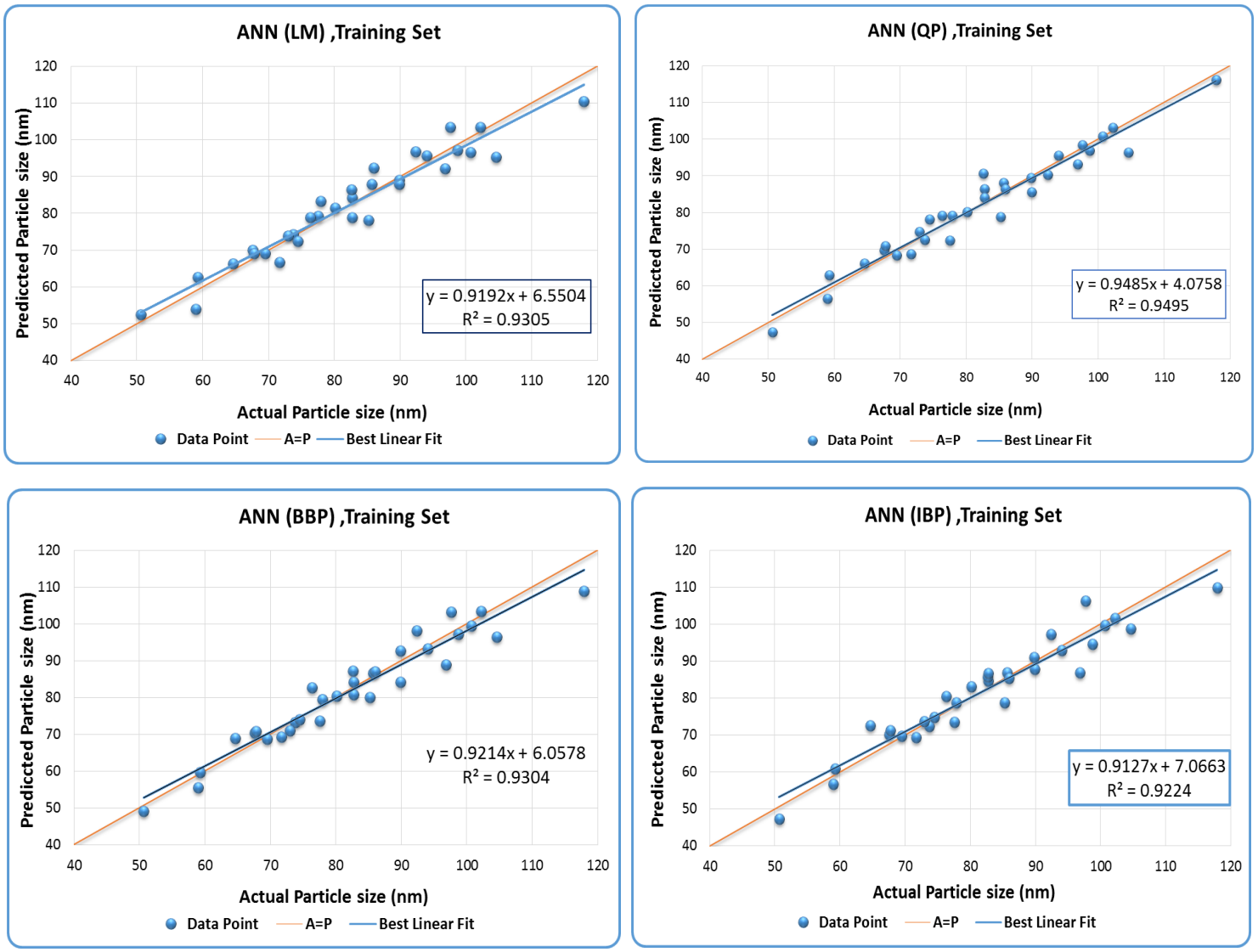

Fig. 4: The scatter plots of the predicted vs. the actual particle size values for the training data set which show the performed R^2 of the optimized topologies, LM-5-7-1, QP-5-13-1, IBP-5-13-1, and BBP-5-14-1.

Table 3: The performance results of the optimized topologies, LM-5-7-1, QP-5-13-1, IBP-5-13-1, and BBP-5-14-1on the particle size of the formulated nanoemulsion.

Learning algorithm	*Architecture*	*Training data*			*Testing data*		
		RMSE	R^2	AAD	RMSE	R^2	AAD
LM	5-7-1	3.91	0.930	3.86	2.50	0.961	2.60
QP	5-13-1	3.33	0.949	3.34	2.03	0.973	2.32
IBP	5-13-1	4.13	0.922	3.89	1.82	0.978	2.16
BBP	5-14-1	3.93	0.930	3.66	1.59	0.984	1.83

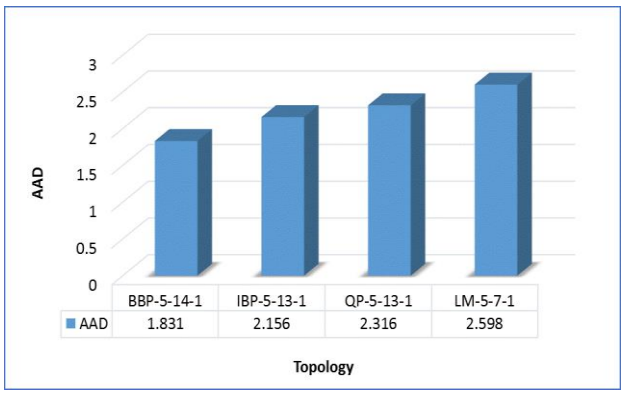

Fig. 5: The AAD values of the selected topologies in testing data set.

The network of BBP-5-14-1

Fig. 6 revels the network of BBP-5-14-1 as a final model for nanoemulsion system which consists of input, hidden, and output layers. The input layer with 5 nodes (percentage of azithromycin, lecithin, Tween 80, glycerol, and vitamin E) is the distributor for the hidden layer with 14 nodes which were determined by learning process.

The input data of hidden nodes are calculated by weighted summation. Then the output data of the hidden layer are transferred to output layer (particle size) using log-sigmoid function.

$$S = \sum_{i=1}^{n} (b - W_i I_i) \qquad (6)$$

where S is the summation, b is a bias, I_i is the ith input to the hidden neuron and W_i is the weight associated with I_i. The bias shifts the space of the nonlinearity properties [22].

$$f(x) = \frac{1}{1 + exp(-x)} \qquad (7)$$

where $f(x)$ is the hidden output neuron. As a result, BBP-5-14-1 was used to determine the optimum as well as the importance values of the input variables of nanoemulsion system in order to achieve the desirable particle size.

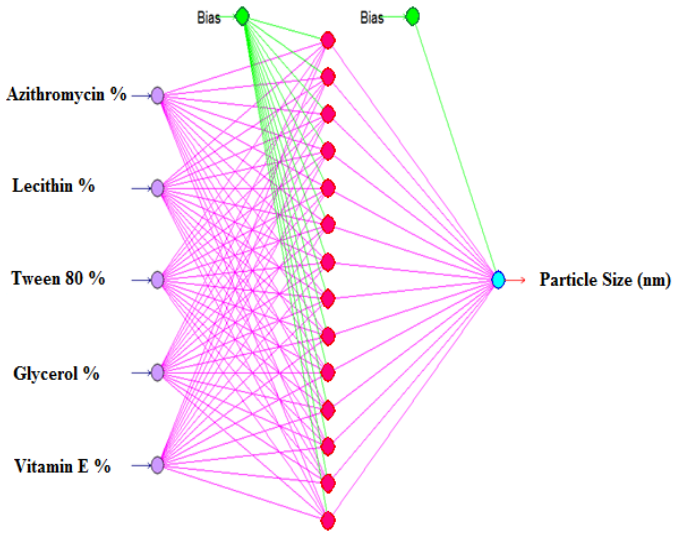

Fig. 6: The network architecture (5-14-1) of the multilayer normal feed-forward connection type of Batch Back Propagation algorithm which consist of 5, 14, and 1nodes in input, hidden and output layer, respectively.

Verification of the model

The optimum azithromycin loaded nanoemulsion was achieved with a composition of 1.4% azithromycin, 2% lecithin, 2% Tween 80, 2.5% glycerol, and 0.25% vitamin E. With these optimum compositions, the predicted particle size value was 53.9 nm. The predicted and actual values were compared to check the adequacy of ANN analysis **(Table 4)**. No significant difference was noted between the experimentally observed and the theoretically predicted particle size values. The sufficiency of the corresponding ANN model was verified based on this observation.

Table 4: The optimized effective variables, model prediction and actual particle size of nanoemulsion system.

Method	*Independent Variables*					*Particle Size (nm)*		
	Azithromycin %	**Lecithin %**	**Tween 80 %**	**Glycerol %**	**Vitamin E %**	**Actual Value**	**Predicted Value**	**RSE (%)**
ANN-BBP	1.4	2	2	2.5	0.25	54.7 ± 0.8	53.9	1.32

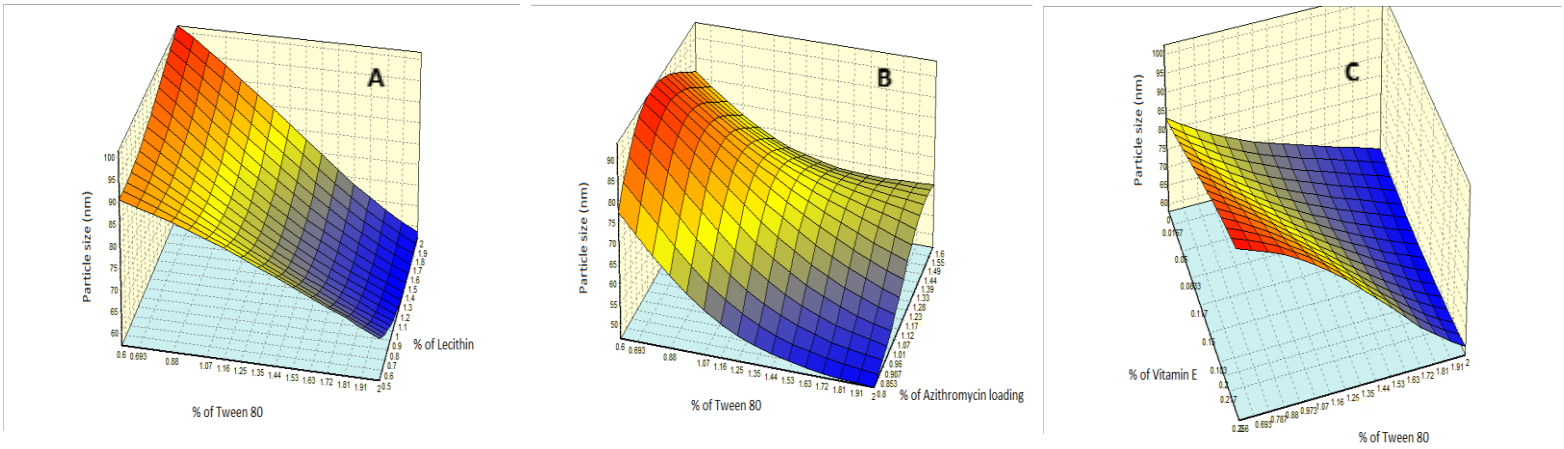

Fig. 7: Predicted response surface plots illustrating the interactive effects of input variables on average particle size of azithromycin- loaded nanoemulsion 4E, (A): effect of % of lecithin surfactant, (B): % of drug loading, (C): % of vitamin E.

The variables' graphical optimization

The validated model (BBP-5-14-1) simulated the influence of the effective variables on the particle size of nanoemulsion system without further need for mathematic knowledge. The simulations demonstrate the impact of non-linear relationship of two variables on the response (particle size) while keeping other variables constant at optimum conditions and are represented graphically by a three dimensional plots **(Fig. 7)**.

Fig. 7 (A) demonstrates the interactive effect of surfactant concentration lecithin and co-surfactant Tween 80 on particle size. A decrease in particle size with increasing surfactant concentrations is well established in the literatures. The results obtained in this study recorded a decrease in particle size of azithromycin- loaded nanoemulsions with increasing surfactant and co-surfactant concentrations. The average particle size decreased significantly when the concentration of Tween 80 was increased giving the lowest particle size at the highest concentration of Tween 80 (2%). Similarly; increasing lecithin concentration reduced the particle size giving the optimum size in a range of 1.2- 2% in the presence of 2% Tween 80. This phenomena could be attributed to excess amount of surfactant molecules adsorbed to oil/ water interface lowering the interfacial tension and reducing the Laplace pressure, thereby facilitating the formation of smaller oil droplets [23, 24]. Furthermore, at higher surfactant levels, excess surfactant molecules will be available to efficiently cover the surfaces of the freshly formed oil droplets during homogenization, thus reducing droplets coalescence rate [25] and favoring droplet breakup process. Regarding the influence of Tween 80 % and drug loading on nanoemulsion particle size; **Fig. 7 (B)** reveals that increasing drug loading resulted in notable increase in particle size (at highest levels of Tween 80) with minimum particle size recorded at the lowest drug loading 0.8% and the highest Tween 80 concentration 2%. This observation could be presumably due to the incorporation of more drug molecules in the oil core that lead to the formation of larger entities.

Additionally, the drug may also exhibits amphiphilic properties that portion of drug molecules may merge themselves as spacer into the surfactant/ co-surfactant monolayer at the interface between oil and aqueous phases producing a rise in particle size [26]. Despite the fact that increase in drug loading led to increase in nanoemulsion particle size, yet; maximum drug loading of 1.4% was chosen in the current study since commercially as well as therapeutically it is often essential to improve loading capacity of nanoemulsion- based delivery systems. **Fig. 7 (C)** shows the effect of vitamin E % and Tween 80 % on particle size. It is evident from the plot that at low concentrations of Tween 80, increment in vitamin E concentration (from 0% to 0.27 %) led to moderate increase in particle size which could be related to the effect of vitamin E on the viscosity of nanoemulsion. It is well known that the higher the viscosity of oil phase; the more difficult and inefficient the disruption of oil droplets within high pressure homogenization is, consequently; oil droplets break-up rate will be more restricted leading to creation of larger droplets [27] [28] and [29]. With the increase in Tween 80 concentration, particle size decreases most probably due to their ability to decrease the interfacial tension between the oil and aqueous phases [30].

Importance of the effective variables

The validated model has determined the relative importance of the nanoemulsion system effective variables at optimum condition **(Fig. 8)**. As shown, Tween 80 exerts the highest influence on the nanoemulsion system formulation with a relative importance of 29.47%. However, the effect of other variables such as percentage of azithromycin, lecithin, glycerol, and vitamin E were quite strong on the particle size as well. Thus, none of the variables was negligible in this work.

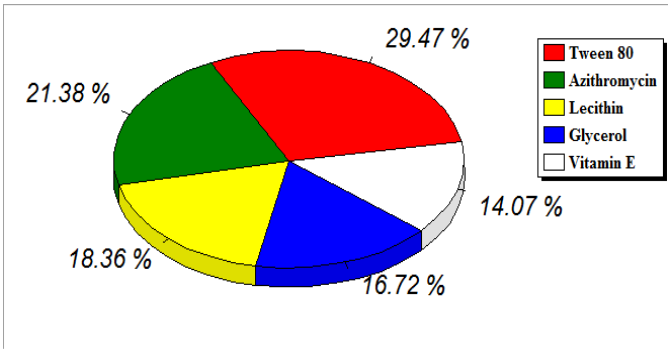

Fig. 8: The relative importance of the nanoemulsion formulation input variables, percentage of azithromycin, lecithin, Tween 80, glycerol, and vitamin E.

Azithromycin-Loaded Nanoemulsions' Stability Assessment

Physical Stability during Storage:

For therapeutic as well as commercial applications, it is often critical that nanoemulsion- based delivery systems remain physically stable throughout storage, transport, and administration. The physical appearance, particle size, PDI, zeta-potential, pH, osmolality, as well as viscosity are the main parameters used to evaluate the physical stability of nanoemulsion formulations and these were employed in this study. Storage stability of azithromycin- loaded nanoemulsions at room temperature (25˚C ± 1˚C) and under extreme conditions (4˚C ± 1˚C and 45˚C ± 1˚C) over a period of 12 months was monitored. 4, 25, and 45˚C were chosen to represent cooling conditions, ambient storage in mild climates, and storage in warm climates, respectively. Particle size, polydispersity index, and zeta potential were determined during this period of storage. Insignificant changes in these parameters indicate nanoemulsion stability.

Fig. 9 depicts particle size of optimized nanoemulsion formulation 4E as a function of time in three different temperatures compared to nanoemulsion 5E **(Fig. 10)**. All azithromycin- loaded nanoemulsions formulated based on the recommended optimum conditions (4E) were highly stable at 4˚C as well as at room temperature during the tested period (12 months). It was noted that nanoemulsions stored at 4˚C were remarkably stable with almost unchanged particle size (from 54.7 nm ± 0.8 on day one to 56.5 nm ± 0.9 on day 360) over the 12 months examination period, whereas for those formulations kept at room temperature (25˚C) the particle size increased up to 62.2 nm ± 5.3. Generally, 4˚C was the most appropriate storage temperature, however; long- term storage at 25˚C did not result in nanoemulsion aggregation, phase separation or drug precipitation compared to 4˚C storage conditions. The good stability could be attributed to the steric stabilizing effect of the non-ionic emulsifier (lecithin) by which a bulk steric barrier is formed preventing particle collision and limiting the occurrence of flocculation and coalescence[12]. However, it was also observed, as expected, that nanoemulsions stored at 45˚C exhibited a notable increase in particle size (from 54.7 nm ± 0.8 up to 106.7 nm ± 3.9). This relatively slow destabilization process may be due (in part) to Ostwald ripening in which big particles grow at the expense of smaller particles due to the higher molecular diffusion of the smaller particles in the continuous phase [31] and because OR is a temperature sensitive phenomena; the increment recorded in particle size were significant at 45˚C [32]. Additionally, up on increasing the temperature water evaporation from the continuous phase will take place which may disrupt the interfacial tension, electrostatic and static repulsions as well as the viscosity of the outer phase leading to significant particle size enlargement. Intravenous administration of large particles may induce several undesirable consequences. First; irritation at the site of injection [33], second; large particles could be recognized by the macrophages in the blood stream which results in rapid removal of nanoemulsion particles from circulation [34].

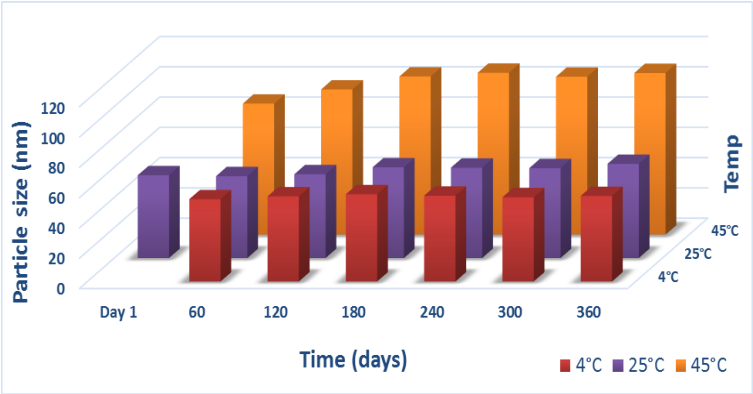

Fig. 9: Long- term stability assessment of optimized nanoemulsion (4E) upon storage under variable temperature conditions (4˚C, 25˚C, and 45˚C). Particle size was measured as a function of time over a period of 12 months. Number of batches per study = 3.

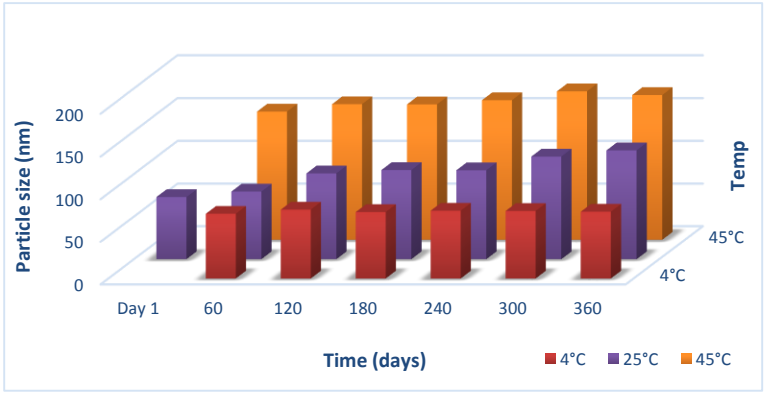

Fig.10: Long- term stability assessment of non- optimized nanoemulsion (5E) upon storage under variable temperature conditions (4˚C, 25˚C, and 45˚C). Particle size was measured as a function of time over a period of 12 months. Number of batches per study = 3.

Third; large nanoemulsion particles are unable to penetrate the BBB efficiently if they are designed to reach the brain cells for targeted therapy [35].Thus; as though no phase separation was observed at the end of the examination storage period, yet those formulations stored at 45˚C are practically considered unaccepted for intravenous administration. **Fig. 10** reveals the results recorded for the stability assessment of azithromycin-loaded nanoemulsions (5E) over 12 months period of storage. Freshly prepared samples possess particle size of 72.9 ± 1.0 nm. Upon storage at 4˚C for 12 months; no appreciable change in particle size was observed (78.5 ± 2.3 nm), whereas keeping the formulations at 25˚C and 45˚C produced a significant increase in size (127.6 ± 4.7 nm, and 169.5 ± 2.6 nm, respectively). Compared to the optimized nanoemulsion (4E), non- optimized nanoemulsion 5E showed a rapid growth in particle size over the examined storage period when the formulated nanoemulsions were kept at 25˚C ± 1˚C and 45˚C ± 1˚C manifesting higher rate of physical instability than that recorded for nanoemulsion 4E. This observation could be explained by the presence of extra free emulsifier in form of micelles in formulations 4E (total surfactant / co-surfactant 4%) compared to formulations 5E (total surfactant mixture 2.5%) that will help improving the stability and preventing coalescence. At 4˚C, both 4E and 5E nanoemulsion formulations were said to have good physical stability since the storage temperature was almost approaching freezing temperature, where by all particles were believed to be in frozen state preserving their properties with slower movement and lower kinetic energy. It is proposed that; upon increasing the temperature, the movement of oil droplets will increase, subsequently their physical contact will also increase leading to higher tendency to flocculation and coalescence [36]. Additionally, the noticeable difference between the stability of the formulation stored at 4˚C and those stored at higher temperatures (25˚C and 45˚C) could be due to alteration in the optimum curvature of surfactant monolayer on account of the progressive dehydration of the hydrophilic head group non-ionic surfactant Tween 80 at higher temperatures which favors an ultralow interfacial tension and promotes droplet coalescence [37]. Furthermore; this process decreases the hydration repulsion among oil droplets allowing them to aggregate with each other's. Similar results were reported by Rao and McClements in their study [Food-grade microemulsions, nanoemulsions and emulsions: Fabrication from sucrose mono Palmitate and lemon oil] [38]. Temperature affects the rate of buildup of interface layer by modifying the adsorption rate and interface features. Also influences film compressibility by altering surfactant solubility in the continuous phase promoting for the formation of larger particles [39]. Thus; even though 4E and 5E nanoemulsion formulations were properly stabilized against the coagulation/ coalescence process, OR could still be the cause for their substantial breakdown [40].

Morphological Studies

Particle size determination should utilize at least two complementary techniques since the size ranges usually expand beyond the capacity of detection of any single instrument. For particle size lower than 1µm, dynamic light scattering, electron microscopy both are useful [41]. In order to confirm the DLS data and to gain details about the form and size of nanoemlsion oil droplets, transmission electron microscopy (TEM) was applied **(Fig. 11)**. For size determination, TEM has the utility of direct visualization of each particle, which provide more accurate information about the size, size distribution and more important, the shape of the particles [42]. Additionally, particles other than nanoemulsions if present can be clearly observed in TEM images. When employing TEM technique for the characterization of nanoemulsions, the existence of larger particles is not an entirely uncommon observation [43 44]. When the size of an individual particle was determined for freshly prepared samples with the help of scale bars on the right side of each image, almost all particles were found to be smaller than 100 nm **(Fig. 11)** ranging between (42.2 - 68.1 nm) in size with nearly mono-dispersed and almost spherical shape oil droplets which is closely corresponding to the results obtained by dynamic light scattering (DLS). Therefore, from the view point of particle size and shape; it could be deduced that the optimized nanoemulsion 4E was safe for intravenous administration.

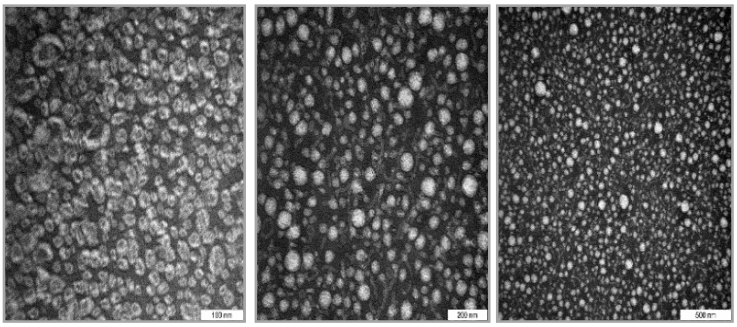

Fig. 11: TEM photomicrographs of freshly prepared azithromycin-loaded nanoemulsion 4E after negative staining with uranyl acetate. The scale bars represent 100, 200, and 500 nm respectively.

Conclusions

The compositions of nanoemulsion system including percentage of each azithromycin, lecithin, Tween 80, glycerol, and vitamin E as effective variables were modeled by ANN to identify the desirable particle size of the optimum nanoemulsion system. To obtain the qualified network, different algorithms were learned using training and testing data sets. The results of the learning program were 4 topologies (LM-5-7-1, QP-5-13-1, IBP-5-13-1, and BBP-5-14-1). The performance of these topologies were optimized by RMSE, R^2, and AAD. The topology (BBP-5-14-1) with the lowest RMSE, AAD and the highest R^2 was chosen as provisional network of the nanoemulsion. The model has determined the optimum values and relative importance of the effective variables. The importance of each variable was Tween 80 (29.47%), azithromycin (21.38 %), lecithin (18.36 %), glycerol (16.72 %), and vitamin E (14.07 %) which indicate that none of the variables is neglect able. The predicted optimum point was azithromycin percentage of 1.4%, lecithin of 2%, Tween 80 of 2%, glycerol of 2.5%, and vitamin E of 0.25% that experimentally performed to obtain actual particle size of (54.7nm ± 0.8). In conclusion, batch back propagation-ANN is an efficient quantitative tool that is capable of modeling the effective input variables to predict the desirable particle size for a stable nanoemulsion system loaded with azithromycin antibiotic.

Conflict of interest statement

The authors have declared no conflict of interest.

Acknowledgment

The authors would like to express deep acknowledgment to Universiti Putra Malaysia for granting this project under Research Grant (RUGs), no. 9199678.

References

1. Ballow, C. H., Amsden, G. W., Martinez, M. D. & Larouche, M. Azithromycin: The first azalide antibiotic. in *Annals of Pharmacotherapy* **26,** 1253–1261 (1992).

2. Lode, H., Borner, K., Koeppe, P. & Schaberg, T. Azithromycin--review of key chemical, pharmacokinetic and microbiological features. *J. Antimicrob. Chemother.* **37 Suppl C,** 1–8 (1996).

3. Hoepelman, I. M. & Schneider, M. M. Azithromycin: the first of the tissue-selective azalides. *Int. J. Antimicrob. Agents* **5,** 145–67 (1995).

4. Codjoe, S. N. A. & Nabie, V. A. Climate change and cerebrospinal meningitis in the Ghanaian meningitis belt. *Int. J. Environ. Res. Public Health* **11,** 6923–6939 (2014).

5. Brouwer, M. C., Tunkel, A. R. & Van De Beek, D. Epidemiology, diagnosis, and antimicrobial treatment of acute bacterial meningitis. *Clinical Microbiology Reviews* **23,** 467–492 (2010).

6. Mace, S. E. Acute Bacterial Meningitis. *Emergency Medicine Clinics of North America* **26,** 281–317 (2008).

7. Van de Beek, D., Brouwer, M. C., Thwaites, G. E. & Tunkel, A. R. Advances in treatment of bacterial meningitis. *Lancet* **380,** 1693–702 (2012).

8. Walsh, F., Amyes, S. G. B. & Duffy, B. Challenging the concept of bacteria subsisting on antibiotics. *Int. J. Antimicrob. Agents* **41,** 558–63 (2013).

9. McIntyre, P. B., O'Brien, K. L., Greenwood, B. & Van De Beek, D. Effect of vaccines on bacterial meningitis worldwide. *The Lancet* **380,** 1703–1711 (2012).

10. Musa, S. H. *et al.* Formulation optimization of palm kernel oil esters nanoemulsion-loaded with chloramphenicol suitable for meningitis treatment. *Colloids Surfaces B Biointerfaces* **112,** 113–119 (2013).

11. Basri, M. *et al.* Comparison of estimation capabilities of response surface methodology (RSM) with artificial neural network (ANN) in lipase-catalyzed synthesis of palm-based wax ester. *BMC Biotechnol.* **7,** 53 (2007).

12. Olivieri, A. C. Practical guidelines for reporting results in single- and multi-component analytical calibration: a tutorial. *Anal. Chim. Acta* **868,** 10–22 (2015).

13. Zainol, S. *et al.* Formulation optimization of a palm-based nanoemulsion system containing levodopa. *Int. J. Mol. Sci.* **13,** 13049–13064 (2012).

14. Pendashteh, A. R. *et al.* Modeling of membrane bioreactor treating hypersaline oily wastewater by artificial neural network. *J. Hazard. Mater.* **192,** 568–575 (2011).

15. Fard Masoumi, H. R. *et al.* Optimization of process parameters for lipase-catalyzed synthesis of esteramines-based esterquats using wavelet neural network (WNN) in 2-liter bioreactor. *J. Ind. Eng. Chem.* **20,** 1973–1976 (2014).

16. Abdollahi, Y. *et al.* Fabrication modeling of industrial CO2 ionic liquids absorber by artificial neural networks. *J. Ind. Eng. Chem.* (2014). doi:10.1016/j.jiec.2014.10.029

17. Ma, C. G. & Weng, H. X. Application of Artificial Neural Network in the Residual Oil Hydrotreatment Process. *Pet. Sci. Technol.* **27,** 2075–2084 (2009).

18. Abdollahi, Y. *et al.* Artificial neural network modeling of p-cresol photodegradation. *Chem. Cent. J.* **7,** 96 (2013).

19. Amani, A., York, P., Chrystyn, H. & Clark, B. J. Factors affecting the stability of nanoemulsions-use of artificial neural networks. *Pharm. Res.* **27,** 37–45 (2010).

20. Li, J., Cheng, J., Shi, J. & Huang, F. Brief Introduction of Back Propagation (BP) Neural Description of BP Algorithm in Mathematics. **2,** 553–558 (2012).

21. Krogh, A. What are artificial neural networks? *Nat. Biotechnol.* **26,** 195–197 (2008).

22. Khataee, A. R. Photocatalytic removal of C.I. Basic Red 46 on immobilized TiO2 nanoparticles: artificial neural network modelling. *Environ. Technol.* **30,** 1155–68 (2009).

23. Qian, C. & McClements, D. J. Formation of nanoemulsions stabilized by model food-grade emulsifiers using high-pressure homogenization: Factors affecting particle size. *Food Hydrocoll.* **25,** 1000–1008 (2011).

24. Ngan, C. L. *et al.* Comparison of Box-Behnken and central composite designs in optimization of fullerene loaded palm-based nano-emulsions for cosmeceutical application. *Ind. Crops Prod.* **59,** 309–317 (2014).

25. Ziani, K., Chang, Y., McLandsborough, L. & McClements, D. J. Effect of particle charge on the antifungal properties of thyme oil nanoemulsions. in *85th ACS Colloid and Surface Science Symposium, Montreal, QC, Canada, June 19-22* COLLSYMP–256 (2011).

26. Sakeena, M. H. F., Elrashid, S. M., Munavvar, a S. & Azmin, M. N. Effects of oil and drug concentrations on droplets

size of palm oil esters (POEs) nanoemulsion. *J. Oleo Sci.* **60,** 155–158 (2011).

27. Ziani, K., Fang, Y. & McClements, D. J. Encapsulation of functional lipophilic components in surfactant-based colloidal delivery systems: Vitamin E, vitamin D, and lemon oil. *Food Chem.* **134,** 1106–1112 (2012).

28. Fredrick, E., Walstra, P. & Dewettinck, K. Factors governing partial coalescence in oil-in-water emulsions. *Advances in Colloid and Interface Science* **153,** 30–42 (2010).

29. Jafari, S. M., Assadpoor, E., He, Y. & Bhandari, B. Re-coalescence of emulsion droplets during high-energy emulsification. *Food Hydrocolloids* **22,** 1191–1202 (2008).

30. Gharibzahedi, S. M. T., Mousavi, S. M., Hamedi, M. & Ghasemlou, M. Response surface modeling for optimization of formulation variables and physical stability assessment of walnut oil-in-water beverage emulsions. *Food Hydrocoll.* **26,** 293–301 (2012).

31. Capek, I. Degradation of kinetically-stable o/w emulsions. *Adv. Colloid Interface Sci.* **107,** 125–155 (2004).

32. Ragelle, H. *et al.* Nanoemulsion formulation of fisetin improves bioavailability and antitumour activity in mice. *Int. J. Pharm.* **427,** 452–459 (2012).

33. Of, E. *et al.* EFFECT OF OIL PHASE CONCENTRATION ON RHEOLOGICAL PROPERTIES AND STABILITY OF BEVERAGE EMULSIONS Elżbieta Dłużewska, Anna Stobiecka, Magdalena Maszewska. (2006).

34. Liu, D., Mori, A. & Huang, L. Role of liposome size and RES blockade in controlling biodistribution and tumor uptake of GM1-containing liposomes. *Biochim. Biophys. Acta* **1104,** 95–101 (1992).

35. Zhu, T. F. & Szostak, J. W. Preparation of large monodisperse vesicles. *PLoS One* **4,** (2009).

36. Eid, A. M. M., Elmarzugi, N. A. & El-Enshasy, H. A. Preparation and evaluation of olive oil nanoemulsion using sucrose monoester. *Int. J. Pharm. Pharm. Sci.* **5,** 434–440 (2013).

37. McClements, D. J. Nanoemulsions versus microemulsions: terminology, differences, and similarities. *Soft Matter* **8,** 1719 (2012).

38. Rao, J. & McClements, D. J. Food-grade microemulsions, nanoemulsions and emulsions: Fabrication from sucrose monopalmitate & lemon oil. *Food Hydrocoll.* **25,** 1413–1423 (2011).

39. Henry, J. V. L., Fryer, P. J., Frith, W. J. & Norton, I. T. The influence of phospholipids and food proteins on the size and stability of model sub-micron emulsions. *Food Hydrocoll.* **24,** 66–71 (2010).

40. Sadtler, V. M., Imbert, P. & Dellacherie, E. Ostwald ripening of oil-in-water emulsions stabilized by phenoxy-substituted dextrans. *J. Colloid Interface Sci.* **254,** 355–361 (2002).

41. Floyd, A. G. Top ten considerations in the development of parenteral emulsions. *Pharmaceutical Science and Technology Today* **2,** 134–143 (1999).

42. Klang, V., Matsko, N. B., Valenta, C. & Hofer, F. Electron microscopy of nanoemulsions: An essential tool for characterisation and stability assessment. *Micron* **43,** 85–103 (2012).

43. Hatanaka, J. *et al.* Physicochemical and pharmacological characterization of alpha-tocopherol-loaded nano-emulsion system. *Int. J. Pharm.* **396,** 188–193 (2010).

44. Preetz, C., Hauser, A., Hause, G., Kramer, A. & Mäder, K. Application of atomic force microscopy and ultrasonic resonator technology on nanoscale: Distinction of nanoemulsions from nanocapsules. *Eur. J. Pharm. Sci.* **39,** 141–151 (2010).